92-GT-61

THE AMERICAN SOCIETY OF MECHANICAL ENGINEERS
345 E. 47 St., New York, N.Y. 10017

Three Dimensional Transonic Flow Measurements in an Axial Turbine with Conical Walls

F. KOST
DLR-Institute for Experimental Fluid Mechanics
Bunsenstr. 10, W-3400 Göttingen, Germany

ABSTRACT

To investigate the spatial flow structure caused by sweep and dihedral effects in turbomachinery blade rows, detailed measurements have been conducted in the windtunnel for rotating annular cascades of DLR-Göttingen. The special configuration investigated, consisted of a turbine rotor equipped with straight blades, a conical hub and a conical casing with a cone half-angle of 30°. Numerous flow data are obtained from surface pressure distributions at seven radial blade sections and from Laser velocimetry upstream, downstream and inside the rotor. As the Laser-Two-Focus technique is a two-dimensional one, two laser velocity measurements at different angles had to be taken at each meaurement location in the flow, in order to get the three components of velocity. The measurement accuracy of the three derived Mach number components in the blade relative system has been evaluated and stored together with mean and fluctuating values at each measurement location.

NOMENCLATURE

h	height above hub
l	profile chord length
t	blade pitch
x, y, z	cartesian coordinates (blade rotating axial system)
x, φ, r	cylindrical coordinates
Ma	Mach number
p	pressure
T	temperature
u, v	absolute velocity (-components)
w	relative velocity
α	absolute flow angle (measured from circumferential direction)
β	relative flow angle, calculated from axial and circumferential component (see fig. 2)
β_s	stagger angle
κ	ratio of specific heats
R	specific gas constant
σ	conical angle, calculated from axial and radial component
ω	rotor angular speed

Subscripts

0	total flow conditions
1,2	inlet, outlet plane
k	profile contour
is	isentropic
x, m	axial, meridional
r, φ	radial, circumferential
w	relative system

Superscripts

-	time mean value
'	instationary part

INTRODUCTION

The development of modern high-power axial turbines has led to increasing pressure ratios across the stage. The resulting density ratios now often require a considerable increase of the annulus cross section in flow direction. Therefore especially in the rear stages of low-pressure steam turbines and in high-pressure turbines of jet engines the casing may be conical with cone half-angles up to 40°.

Presented at the International Gas Turbine and Aeroengine Congress and Exposition
Cologne, Germany June 1-4, 1992

The intersection of a conical stream surface with a blade leads to significant amounts of sweep and dihedral, even when the staggered blades themselves are radial. Theoretical and experimental results for incompressible and subsonic flows of such kind were published for example from Hill and Lewis (1974), Graham and Lewis (1974), Gotthardt (1983) and Potts (1987). As these flows are especially important in transonic flow regime, an experimental investigation was started in Göttingen, using a rotating annular cascade, to gather more realistic information on the influence of conical angle on aerodynamic characteristics of different turbine blades (Bräunling, 1985; Bräunling and Lehthaus, 1986). Mainly conventional probe measurements upstream and downstream of different test wheels were carried out, together with measurements of blade pressure distributions and some 3D-Euler calculations (Lehthaus, 1983). The results of the experimental investigation did not allow to derive a general correlation between the losses and the conical angle, nevertheless a continuous increase of losses with increasing conical angle was predicted. But a physical explanation of the observed loss behaviour could not be given.

Sweep and dihedral effects are well known from the aerodynamics of single airfoils. Fluid particles adjacent to the suction and pressure side of the blade trace out different paths, the sweep angles computed from spanwise and axial components are different on both side. In a turbine this gives rise to periodically twisted stream surfaces at the exit of the blade row (Smith and Yeh, 1963). One possible explanation of the loss rise is the change in the pressure distribution when the flow changes from cylindrical to conical conditions. In a theoretical approach it would at first be necessary to calculatate the pressure distribution. Potts (1987) or Lehthaus (1983) have shown that a 3D calculation is necessary to achieve a sufficient agreement with a measured pressure distribution. By 2D computations it is only possible to get approximate results at mid section of the blade. There are two possible methods of looking at conical flows by the application of 2D calculation methods. The "section method" assumes that the flow strictly remains in a conical plane equivalent to the cylindrical plane often assumed in turbine design methods. A better description of the flow behaviour is achieved by the "projection method". The "projection method" (Hill and Lewis, 1974; Gotthardt, 1983), based upon infinite span of the swept blade, explains the observed flow features by the vector addition of a constant spanwise velocity and the two-dimensional velocity field of the blade section normal to the spanwise direction.

In incompressible flow, at the trailing edge the velocities of fluid particles coming from the pressure respectively from the suction side of the blade have equal amount and direction. Therefore, in a calculation using the projection method, which assumes constant spanwise velocity (at least in a plane of constant x), downstream of the trailing edge no additional vortex sheet is caused by the twist of the stream surfaces. But already the experimental results of Gotthardt (1983) in incompressible flow show that the radial velocities of fluid particles coming from pressure and suction side do not coincide. In compressible flow, there is still more reason to expect a jump in the radial velocities at the trailing edge as flow theory requests only equal pressures but not equal velocities there. That is why a real transonic conical flow through a row of finite blades should exhibit extra shed vorticity downstream of the trailing edge, which has its origin in the different local conical angles of the fluid coming from the pressure respectively from the suction side. This means, an additional mechanism giving rise to trailing shed vorticity exists in conical flow. The additional vorticity is a second possible reason of the increase of losses with conical angle.

Of course, streamwise vorticity is also caused by normal wall-boundary-layer induced secondary flow and by secondary flow that has its origin in changing profile loading across the span. To separate the different mechanisms which may lead to the observed loss behaviour and in order to get a better understanding of high speed conical flows it was decided that the detailed investigation of the spatial flow stucture of at least one specific transonic configuration should be conducted.

TEST FACILITY AND TEST CONFIGURATION

The tests were carried out in the windtunnel for rotating annular cascades of the DLR, Göttingen. The test section comprises an annular cascade but instead of giving a relative inlet angle different from 90° by preswirl, the absolute flow in the tunnel is without swirl and the relative angle is adjusted by the speed of the test wheel. The rotor scrapes itself into an abrasive material so there should be no tip clearance. The hub is not rotating ahead and behind the rotor. A complete description of the tunnel and the more conventional measurement methods like probe measurements and blade surface pressure measurements (on the rotating wheel) was reported by Bräunling (1985). The specific configuration, tested in more detail here, is also one of those configurations, results on which have been reported by Bräunling and Lehthaus.

The actual configuration consisted of a turbine rotor equipped with 80 straight blades, a conical hub and a conical casing with a cone half angle of $\sigma = 30°$. In the meridional plane the conical walls are straight parallel lines in the vicinity of the test wheel. In order to get thin wall boundary layers the annulus area exhibits a minimum in front of the rotor and was designed with constant area shortly behind the rotor. The measurement points were mainly located in measurement planes. The two probe measurement planes are shown in fig. 1. Table 1 gives their coordinates, together with two more measurement planes, from where results are shown in the paper.

	hub		casing	
	x [mm]	r [mm]	x [mm]	r [mm]
plane 1	-9.0	223.2	-27.0	254.4
$x/l_x = -0.21$	-5.0	225.5	-5.0	267.1
blade entrance	0.0	228.4	0.0	270.0
blade exit	23.64	242.0	23.64	283.6
$x/l_x = 1.48$	35.0	248.6	35.0	289.8
plane 2	60.0	263.7	42.7	293.9

Table 1 : Coordinates of some measurement planes

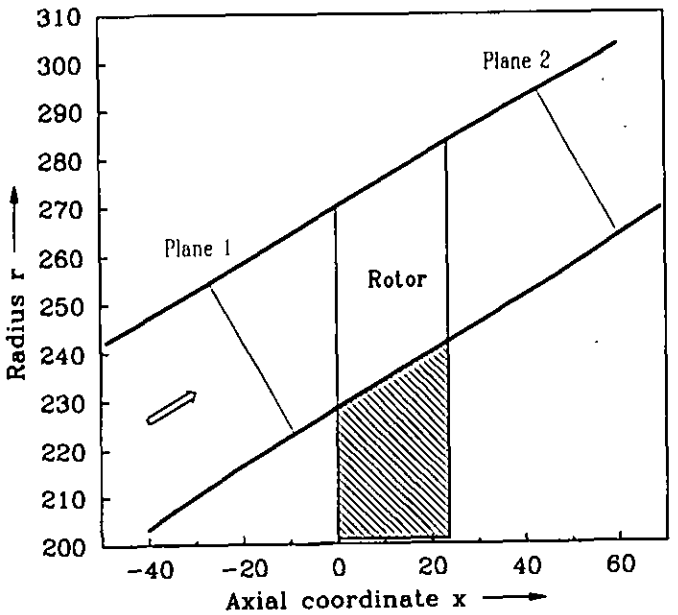

Fig. 1: Test section

Figure 1 shows the meridional plane of the test configuration. Profile and cascade geometry at the mean radius are shown in Fig. 2. The profile coordinates and some results from plane cascade measurements were given by Kiock et al. (1985). Whereas probe and pressure distribution measurements were carried out at a number of flow conditions, the laser velocity measurements were done at just one flow condition. The nominal and the measured mean values determining this special flow condition are listed in table 2. The inlet total pressure profile (absolute system) is plotted in figure 3.

Inlet flow values in plane 1 (absolute system)			
T_{01}	p_{01}	α_1	massflow (integrated)
297 K	26670 Pa	90°	1.609 kg/s

rotor angular speed: ω = (194.3 ± 0.2) rad/s

mean static pressures on the side walls				
	x [mm]	r [mm]	p/p_{01}	
hub	-30.2	209.9	0.936 ± 0.001	
	-9.0	223.2	0.943 ± 0.001	plane 1
	60.0	263.7	0.509 ± 0.010	plane 2
casing	-27.0	254.4	0.936 ± 0.001	plane 1
	42.7	293.9	0.586 ± 0.010	plane 2
	64.6	305.7	0.609 ± 0.010	

Table 2 : Flow condition for L2F-measurements

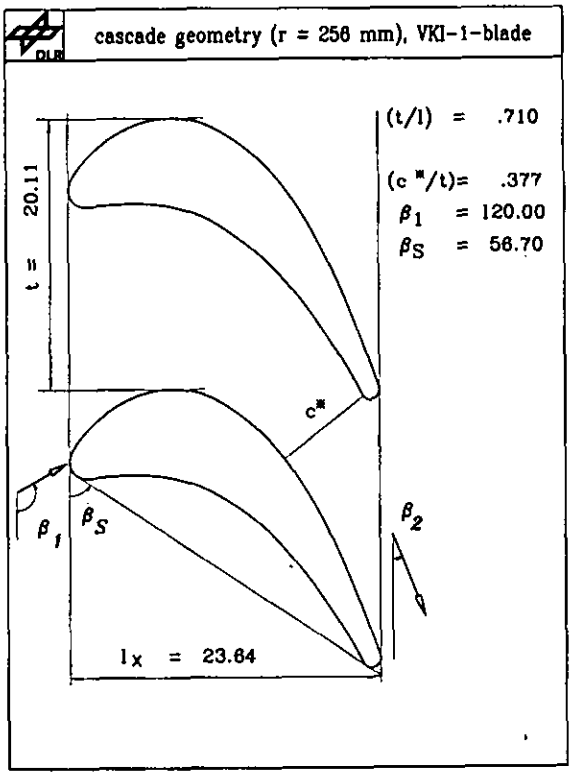

Fig. 2: Profile cascade geometry

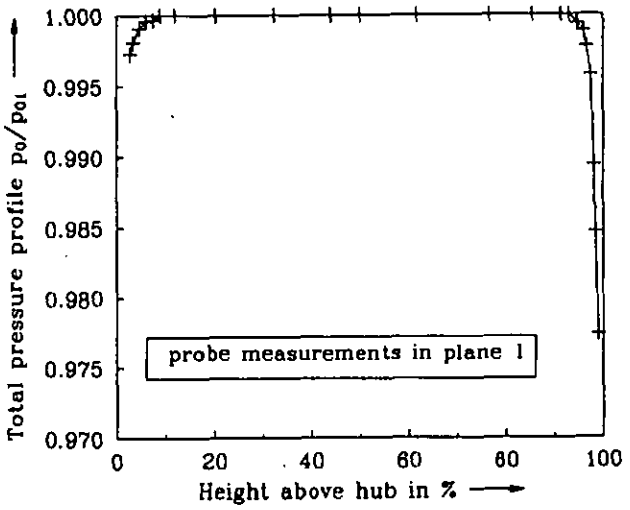

Fig. 3: Inlet total pressure profile

BLADE SURFACE PRESSURE DISTRIBUTION MEASUREMENTS AND RESULTS

Surface pressure distribution measurements in the blade rotating system have been performed at seven blade sections from 5% blade height above the hub to 95% blade height. Each section was a straight line in the meridional plane with a constant conical angle of 30°. In each section 48 pressure tappings were distributed around the profile.

each tapping on a different blade. The position of the tappings can be seen from fig. 4 where the individual results from the tappings are indicated by symbols. The results are not so smooth as measurements in a stationary cascade because transmitting the signals from the rotating to the stationary frame via slip rings introduced some noise.

The quantity plotted in the figures is the isentropic relative contour Mach number Ma_k computed from the measured static pressure on the contour and the calculated isentropic total pressure $p_{0,w,is}$ in the relative system:

$$Ma_k = \sqrt{\frac{2}{\kappa - 1}\left[\left(\frac{p_{0,w,is}}{p}\right)^{\frac{\kappa-1}{\kappa}} - 1\right]} \qquad (1)$$

The isentropic total pressure in the relative system can be calculated at any point in the test section outside the wall boundary layers by using following formula:

$$p_{0,w,is}(r) = p_{01}\left(1 + \frac{\kappa - 1}{2\,\kappa R}\,\frac{\omega^2 r^2}{T_{01}}\right)^{\frac{\kappa}{\kappa-1}} \qquad (2)$$

This formula was derived by exploiting the special features of the tunnel, which are: no inlet swirl ($v_{1\varphi} = 0$), no heat exchange, T_{01} and p_{01} constant in the inlet plane (except in the wall boundary layers).

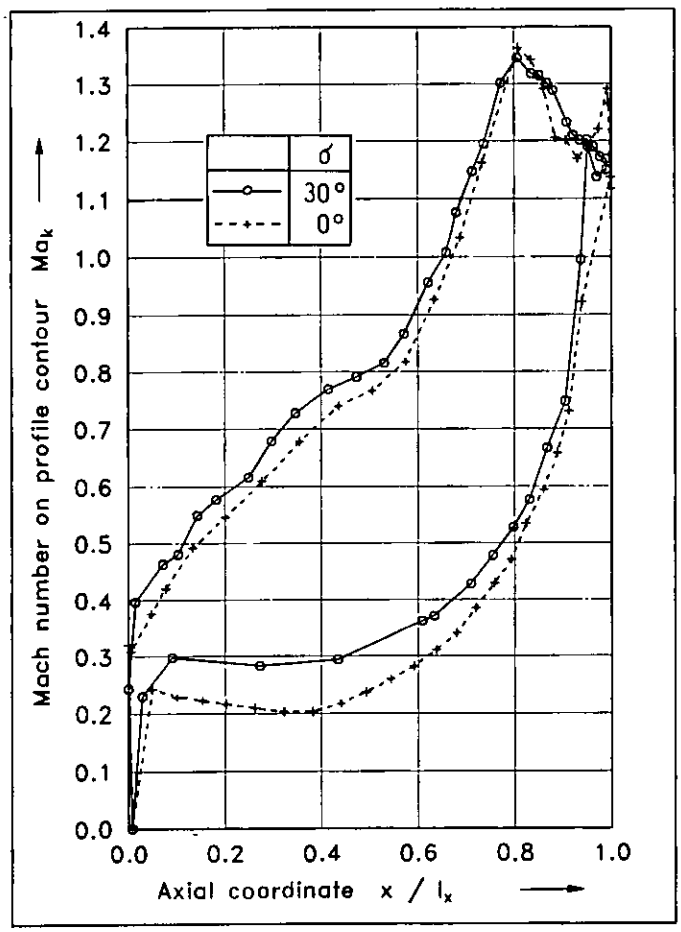

Fig. 4: Comparison of blade surface Mach distributions from the annular (h=50%, $\sigma = 30°$) and plane (unswept) cascade

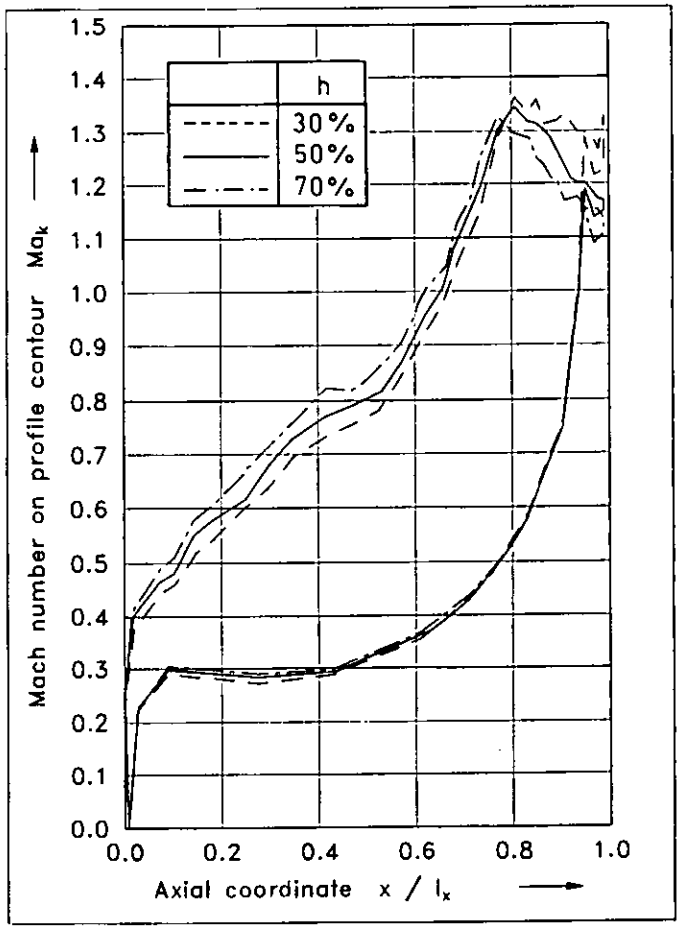

Fig. 5: Profile contour Mach number distribution at blade height h = 30%, 50%, 70%

In fig. 4 the Mach number distribution from the annular cascade is compared with a result from the (unswept) plane cascade (Baines et al., 1985). Both distributions have been measured at the same blade exit Mach number at mid section. That is why the Mach number level nearly coincides in the rear part of the blade, because it is enforced by the downstream pressure. In the front part of the blade the Mach number of the conical measurement is higher than in the plane cascade. This results confirms the general tendency known from the "projection method" which assumes a superposition of a spanwise velocity and the normal 2D velocities. But from the measurement result of course no constant spanwise Mach number component can be derived.

In the following figures Mach number distributions from the annular cascade at different blade heights are shown. The symbols have been omitted to get a clearer visualization of the curves. In fig. 5 the curve from fig. 4 at 50% blade height is compared with results from 30% and 70% blade height. Fig. 6 and 7 show results of the other sections.

In conical flow end walls inevitably induce spanwise variations of the flow values, even when the flow is constant in an inlet plane and friction effects are small. A typical result, which can also be seen in the figures 5 to 7, is the lower profile loading near the hub in the front part of the blade,

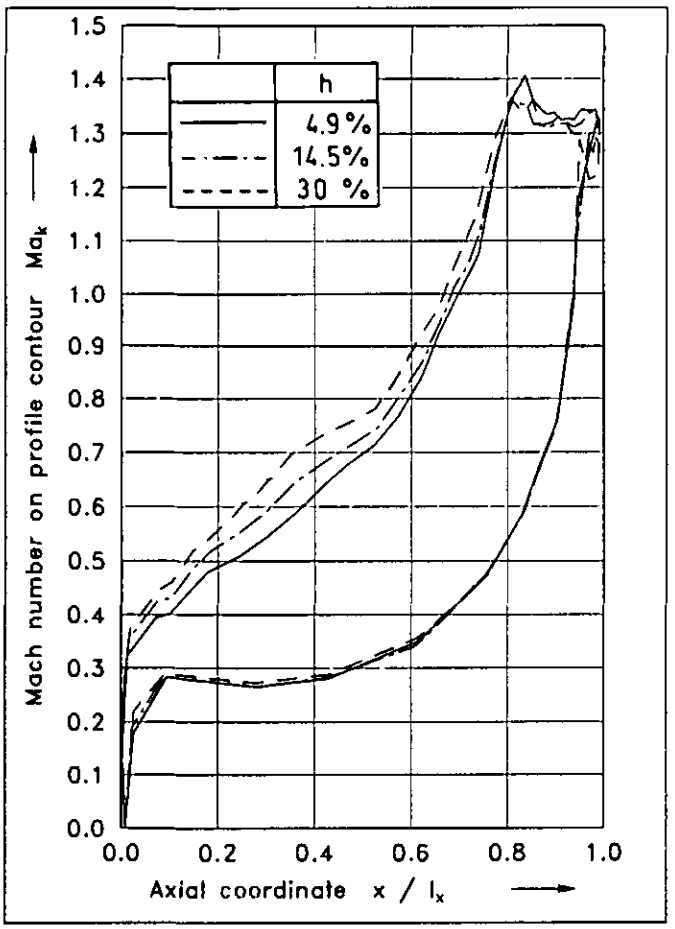

Fig. 6: Profile contour Mach number distribution at blade height h = 4.9%, 14.5%, 30%

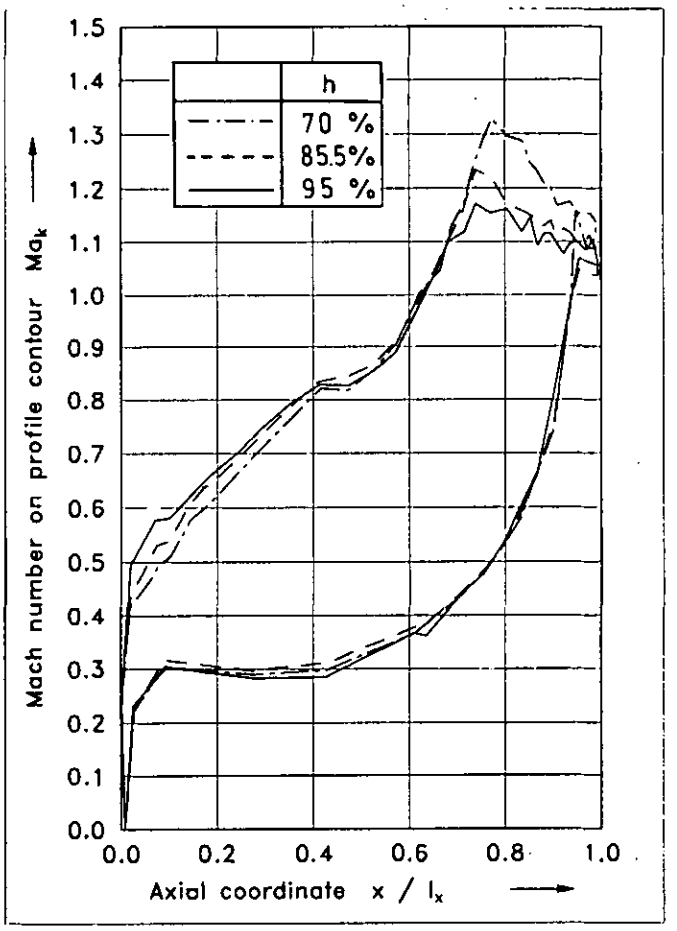

Fig. 7: Profile contour Mach number distribution at blade height h = 70%, 85.5%, 95%

compared to the casing. A good explanation of the spanwise variations generated by conical flow was given by Potts (1987). In the rear part of the blade the variation in profile loading from hub to tip is reversed. This is only partly due to the radial pressure gradient caused by flow swirl, as 3D computations of the flow in the equivalent swept linear cascade (Lehthaus, 1983) gave similar results.

LASER-TWO-FOCUS VELOCIMETRY

To investigate the flow field inside and in the vicinity of the rotor we used a Laser velocimeter of L2F-type as described in detail by Schodl (1980). The L2F-measuring device generates two highly focussed light beams in the probe volume which act as a "light gate" for tiny particles in the flow. The scattered light from the particles provides two successive pulses and from the time interval between the pulses the velocity perpendicular to, but in the plane of the laser beams can be derived. The mean flow angle is provided by turning the second beam around the first and so accumulating time-of-flight histograms at a number of angles. The L2F-measuring device, we used, delivered automatically a time-of-flight histogram integrated over all angle settings and an angle-histogram integrated over all time-intervals. From these two histograms it is possible to compute the mean velocity $\bar{u}$, and the mean angle, $\bar{\alpha}$, in the plane perpendicular to the Laser beams and the turbulence levels in flow direction and perpendicular to it, but it is not possible to get the Reynolds'stress $\overline{u'v'}$. The instrument error in angle is equal to $\overline{u'v'}/\bar{u}^2$. In the present investigation the main error of the L2F-results was the statistical error which results from evaluating a histogram with a finite number of points and finite signal-to-noise ratio. This error was evaluated and stored together with the flow value for every L2F-measurement result. The apparent turbulence level, computed from the histograms seems to be systematically too high by at least 1% (absolute). The reasons of this systematic error seemed to be small variations of flow parameters during the time period of one complete measurement and variations in flow values coming from slight differences between the blade channels. A multi window operation mode as described by Schodl (1980) enabled us to divide every blade pitch into 16 intervals but it was not tried to identify an individual blade on the rotor, that means we assumed strict periodicity.

As the Laser-Two-Focus technique is a two-dimensional one, two laser velocity measurements at different angles had to be taken at each measurement location in the flow, in order ot get the three components of velocity. Additional difficulties then arose from limited optical access to the chosen measurement location and from a kind of astigmalism generated by passing with a converged light beam through a plane window at angles far from perpendicular, which in our case prohibited measurements at angles more than 30°

from the vertical on the window By turning the laser only in a horizontal plane which contained the rotor axis and taking two measurements, the circumferential component of velocity, v_φ, was measured twice and it was possible to gain a new mean circumferential component by computing a weighted mean. Unfortunately, but not unexpected, one realizes that sometimes the difference between the two measured values of v_φ exceeds the sum of the confidence intervals of the two single measurements. In such a case a larger error bar was determined by taking into accout the difference of the values. After the two Laser-measurements at the angle γ_1 and γ_2 (angle between Laser beam and radial direction) the local conical angle σ of the flow can be computed from the two meridional velocity-components v_{m1} and v_{m2} according to following equation:

$$\tan\sigma = \frac{\frac{v_{m1}}{v_{m2}}\cos\gamma_2 - \cos\gamma_1}{\sin\gamma_1 - \frac{v_{m1}}{v_{m2}}\sin\gamma_2} \tag{3}$$

The true meridional component of flow is

$$v_m = \frac{v_{m1}}{\cos(\sigma - \gamma_1)} \tag{4}$$

The total velocity in the relative system is

$$w = \sqrt{v_m^2 + (v_\varphi - \omega r)^2} \tag{5}$$

Because of the above mentioned special features of our tunnel ($v_{1\varphi} = 0$, etc.) one can compute the total temperature in the relative system, T_{0w}, at any point of the flow field:

$$T_{0w}(r) = T_{01} + \frac{\kappa - 1}{2\kappa R}\omega^2 r^2 \tag{6}$$

Now we are able to calculate the Mach number at every measurement point according to:

$$Ma_w = \frac{w}{\sqrt{\kappa R T_{0w} - \frac{\kappa - 1}{2} w^2}} \tag{7}$$

The error bar (equivalent to the 95% confidence-interval) of any stored flow value could be computed by error propagation from the errors of the two single Laser measurements. This is necessary because especially the error of the radial component changes very rapidly in the flow field depending on the number of events in the histogram, on signal-to-noise ratio (a problem in the vicinity of walls), on the flow angle and on the angle difference of the two Laser measurements at the same point.

At a number of axial positions measurements at different radii have been performed. In the presentation of the results some selection has to be made. For more details, see Kost (1992).

RESULTS AT MID SECTION

Figure 8 gives a general view of the flow field at mid section. In the upper two blade channels areas of constant Mach number are plotted, in the lower two areas of constant conical flow angle σ are shown. The lines, separating the flow channels downstream of the blade row, roughly show the wake centre line. It was assumed that downstream of the blade an L2F-histogram with a minimum number of events denotes the position of a measurement point in the wake centre line. Figure 8 could of course only be produced by 2D-interpolation from the L2F-measurement locations. As the Mach number could be measured more accurate than σ and as inside the blade channel the blade surface Mach number could be taken additionally from the pressure distribution, the Mach number plot is much smoother than the σ-plot.

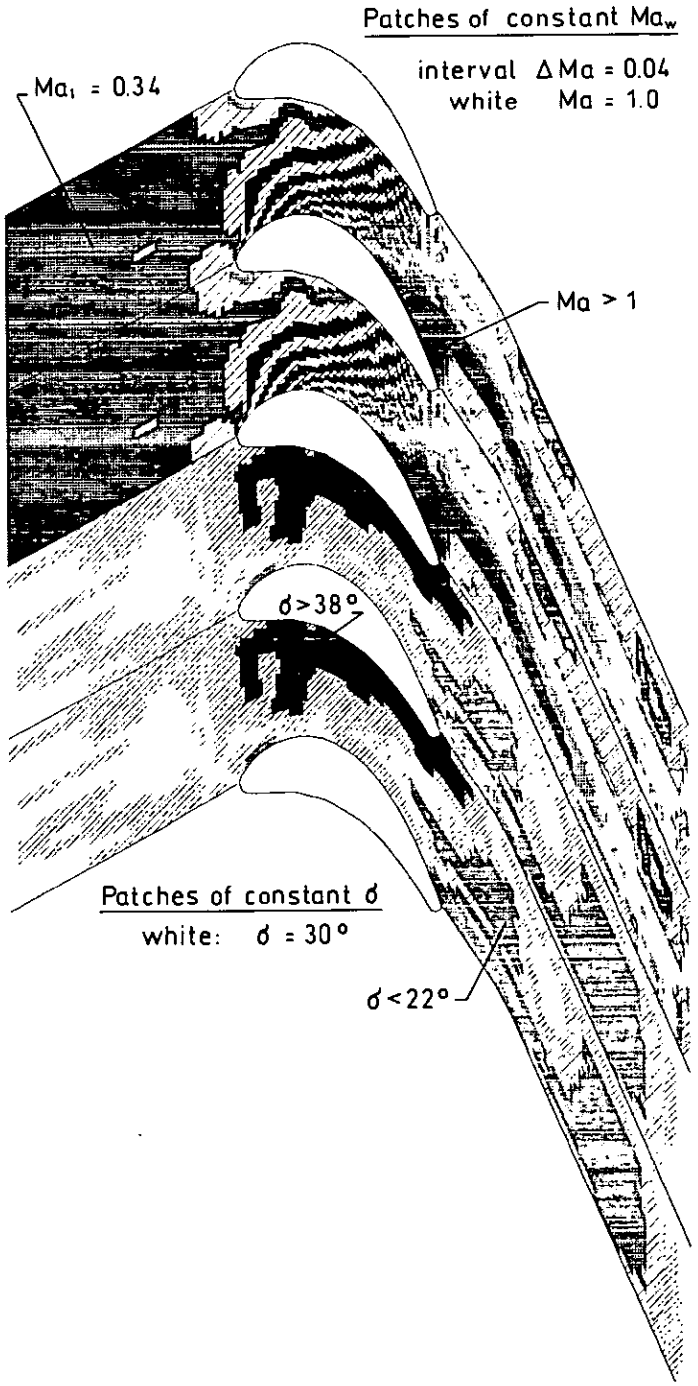

Fig. 8: Flow field at mid section (upper 2 blade channels : Mach lines, lower 2 channels : areas of constant σ)

In subsonic flow single iso-Mach-lines are separated from each other by hatched areas. The areas with sonic flow condition are shown white. Supersonic flow is shown as a single area beginning at the suction side of the blade and extending downstream. As at blade exit the number of measurement points is not sufficient, it is not possible to see the shocks coming from the trailing edge.

In the inlet plane the conical flow angle is 30° as dictated by hub and casing walls. In the blade channel the conical angle is lower than 30° near the suction side and much higher than 30° near the pressure side, the same characteristic feature as found by inviscid calculations, reported by Lehthaus (1983) or Potts (1987).

Next, figure 9 gives selected results at four axial stations in the mid section plane. In these plots the measurement points themselves, together with their respective error bars (when larger than symbol size) are shown. Please note, that $y/t=0$ or $y/t=1$ is the circumferential position of the blade nose in the blade relative system. The gradients of the angle σ are highest at the exit of the blades and in the wakes. It is remarkable that downstream of the blade the variation of the conical flow angle σ is much larger than the variation of the flow angle β, even when the much larger error bars of σ are taken into account.

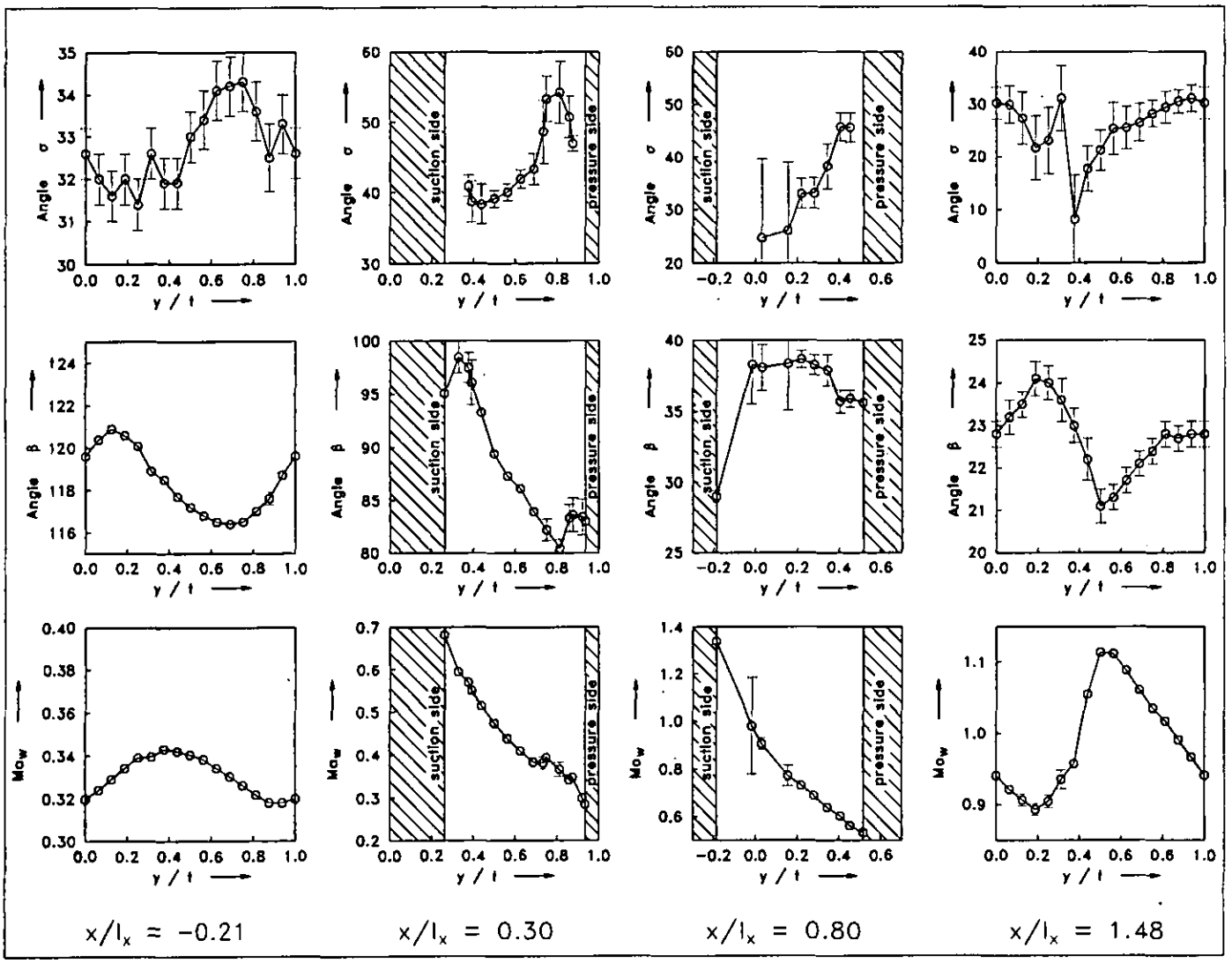

Fig. 9: Results at four axial stations in the mid section plane

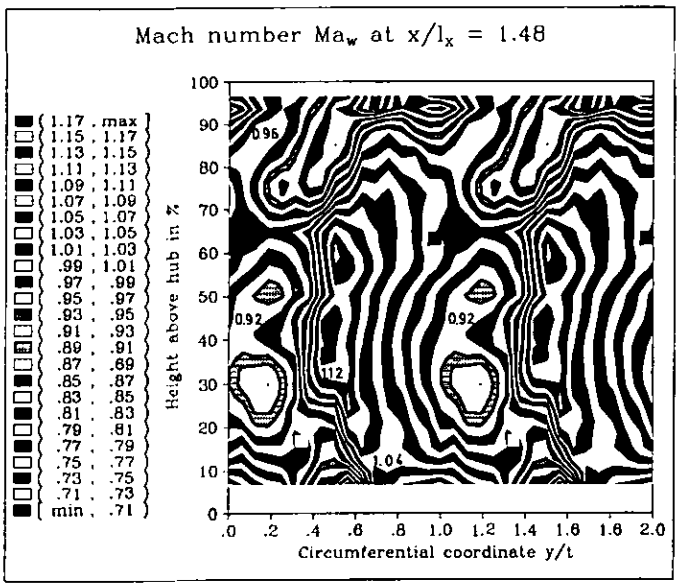

Fig.10: Mach number in a downstream measurement plane

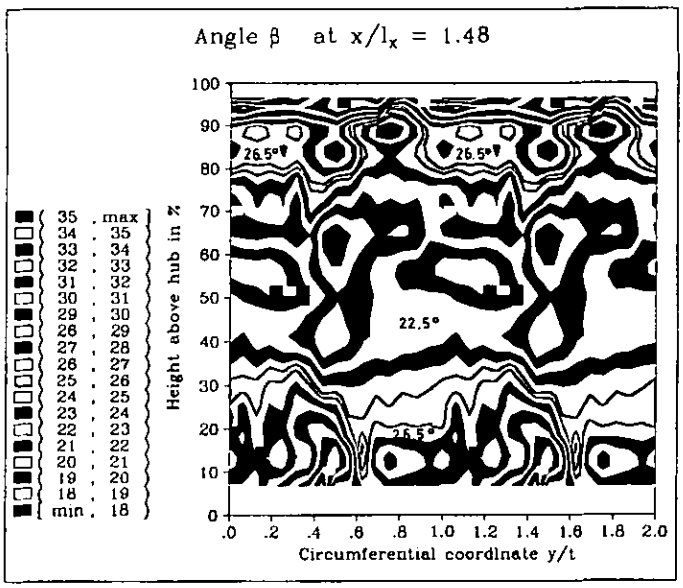

Fig.11: Isocline plot (angle β) in a downstream measurement plane

RESULTS IN A DOWNSTREAM MEASUREMENT PLANE

As an example of the results from a measurement plane an exit plane of constant axial position x/l_x = 1.48 is chosen.

In the Mach number plot (fig. 10) the wake between y/t = 0.0 and 0.4 can be seen and the influence of the radial pressure gradient giving lower Mach numbers near the casing.

The isocline-plot of the angle β (fig. 11) shows mainly that near the walls the turning of the flow is diminished, giving higher angles there. Horizontal lines in the isocline plot with elliptic lines below and above indicate a vortex centre as explained for example by Krain (1987). Therefore the isocline plot gives a hint to several vortex centres : two extended vortices at 25 and 75% height, at the side of the wake coming from the suction side (y/t $\approx$ 0.5) and one smaller but more intense vortex at y/t = 0.8 and h $\approx$ 95% . Two more seem to exist near h $\approx$ 90% : at y/t = 0.1 and y/t = 0.5.

The flow vector plot (fig. 12) has been produced by just taking the measured (not interpolated) Mach number components in circumferential and radial direction, subtracting from them an approximate mean value in the plane, here $Ma_\varphi = 0.8$ and $Ma_r = 0.2$ and plotting the resulting vector. This plot also shows the already mentioned higher flow turning in the mid section outside the wake, furthermore, strong radial components (positive and negative) at the right side of the wake (y/t $\approx$ 0.5) and near hub and casing. Some vortices can be detected in the vector plot, but it is not easy to identify vortices in the plot.

Finally fig. 13 shows the turbulence level in the downstream plane. Of course lower turbulence levels can be seen outside the wake, higher turbulence levels inside the wake. The shift of the wake to higher values of y/t near hub and casing can be explained by the lower turning of the flow there. The very high turbulence level at y/t = 0.8 and h $\approx$ 95% is at the same position as a vortex, detectable in fig. 11 and fig. 12. The vortex is just at the same blade height as the outer edge of the inlet casing boundary layer (see fig. 3). Therefore, it is highly probable that this point of high turbulence, near the suction side of the wake, coincides with a vortex core of wall-induced secondary flow at the casing.

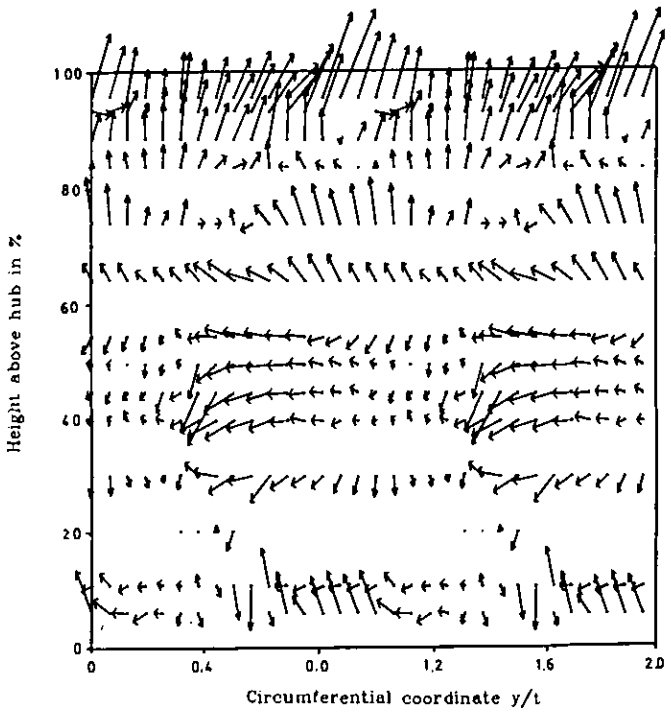

Fig.12: Flow vectors projected into downstream measurement plane, $Ma_\varphi = 0.8$ and $Ma_r = 0.2$ subtracted, at x/l_x = 1.48

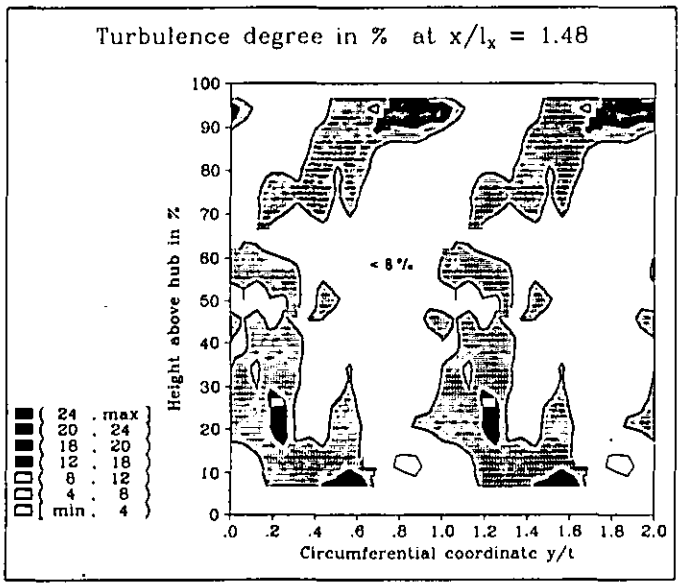

Fig.13: Turbulence in a downstream measurement plane

HOMOGENEOUS DOWNSTREAM FLOW VALUES

From the flow values measured by L2F-technique it was possible to derive the three Mach number components, the flow angles and total temperature. But total pressure has to be measured separately.

We used a fixed pneumatic total pressure probe in order to get the true circumferentially averaged pressure. That is why the total pressure measurement could only be performed in plane 2 (see fig. 1) or further downstream, as nearer to the rotor the probe would not average correctly. From the measured total pressure in the absolute (fixed) system and by using the Mach number, measured by L2F, it is possible to calculate the total pressure in the relative system. A total pressure loss number ζ_w can then be calculated by following formula ($p_{0,w,is}$ from eq. 2):

$$\zeta_w = 1 - \frac{p_{0,w}}{p_{0,w,is}} \qquad (8)$$

Homogeneous flow values can be computed from the measured inhomogeneous values by using the conservation equations (mass, three components of momentum, energy) in an analogous way as Amecke (1970) first applied it to 2D cascade flow. The procedure, used here in 3D flow, is described in detail by Kost (1992).

In fig. 14 the pressure loss in plane 2 together with the homogeneous Mach number and flow angle is plotted. The Mach number and the angle in plane 2 are compared to the mean values of the measurement plane, defined by constant $x/l_x = 1.48$. The Mach number decreases from $x/l_x = 1.48$ to plane 2 because the annulus area is still increasing (see table 1). For the actual configuration Bräunling (1985) found a pressure loss rise of 1.5 % when comparing the cylindrical with the conical flow configuration at mid section. A first guess of the loss rise due to the twisted stream surfaces can be gained by assuming that all kinetic energy normal to the surface of homogeneous σ is lost. At mid section and $x/l_x = 1.48$ a pressure loss rise of 0.5 % is found by this method. Of course, the stated assumption is not strictly valid: part of the kinetic energy may be recovered. A still bigger error results from the fact that part of the velocity-component normal to the surface of homogeneous σ has already been diminished by mixing as fluid passes from the cascade exit to $x/l_x = 1.48$. This means that more than the above stated one third of the loss rise is due to stream surface twist.

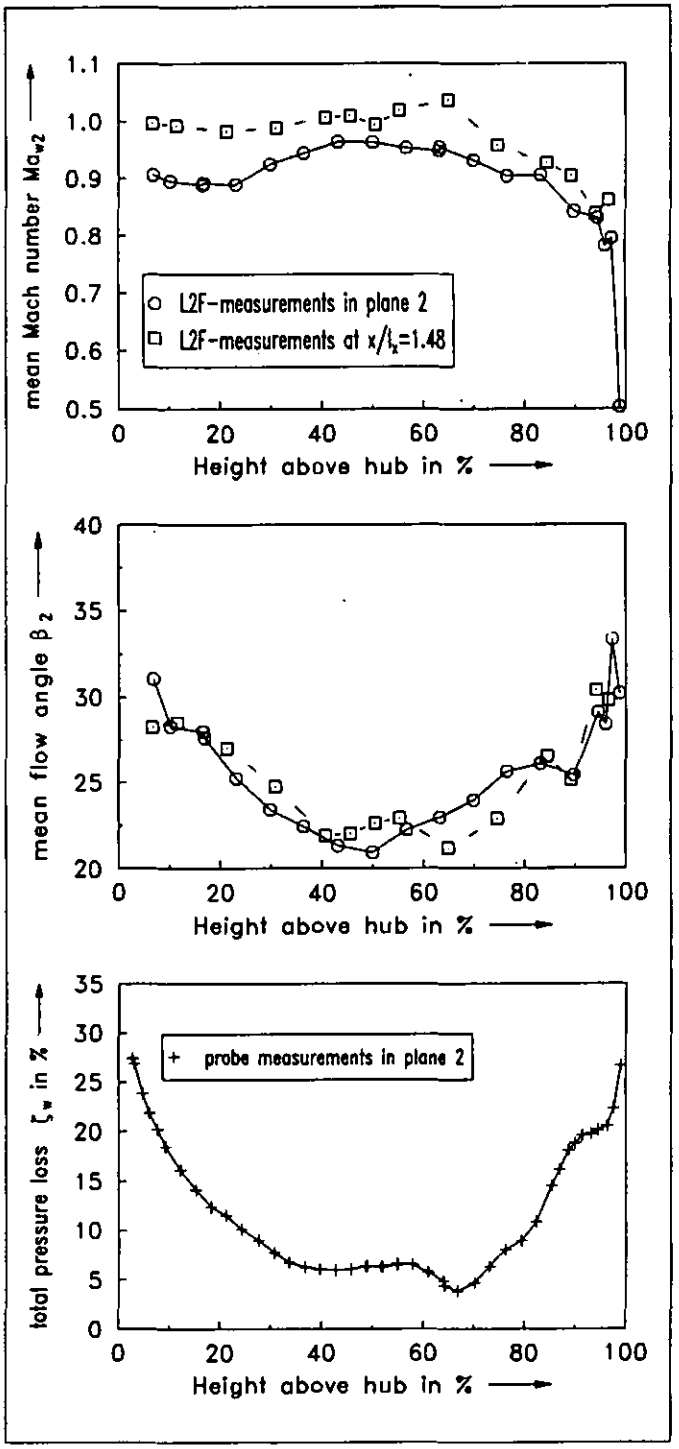

Fig.14: Downstream homogeneous flow values (Mach number, angle, loss)

DISCUSSION

The 3D-measurement results now available for this special case could only be partly analysed and interpreted up to now. In the further investigation of the mid section results, loss contributions have to be analysed more rigorously. A more refined model including boundary layer and trailing edge loss will be necessary to separate the contributions to loss.

The strong 3D-effects, shown in the measurement plane at $x/l_s = 1.48$, to begin 15% below and above the mid section, still need more analysis work to be done. They cannot be explained by normal wall-boundary-layer induced secondary flow which is concentrated near the outside of the inlet wall boundary layer. Secondary flow also arises from changing profile loading in spanwise direction, which is a characteristic of a finite blade in conical flow. Furthermore, the radial velocity component and the rotation of the wheel lead to other types of secondary flow not existing in plane cascade flow and therefore not so broadly investigated. It is planned to make a comparison with an existing 3D Navier-Stokes code and hopefully more questions will be answered than new questions raised.

CONCLUSION

An experimental investigation has been conducted to get some insight into the spatial flow structure, caused by transonic conical flow through an axial turbine. It has been shown that large deviations from an axisymmetric surface exist in conical flow. These deviations produce additional losses.

Inviscid 3D flow calculations as those of Lehthaus (1983) or Potts (1987) are able to reproduce the observed spanwise variations in the blade surface pressure distributions. The downstream spanwise loss variations remain unexplained.

The investigated configuration is characterized by rather simple boundary conditions : homogeneous inlet flow with no swirl in the absolute system, straight blades, very small tip leakage (nominal zero). Nevertheless, it results in a complicated 3D velocity field. There exist a number of measurement points together with individual error bars. Therefore, I think it would be of great interest to compare the measurements with numerical predictions.

ACKNOWLEDGEMENTS

The author wishes to thank Mr. Schüpferling and Mr. Tappe for maintaining and running the tunnel during these lengthy measurements.

REFERENCES

Amecke, J., 1970, "Anwendung der transsonischen Ähnlichkeitsregel auf die Strömung durch Ebene Schaufelgitter", *VDI-Forschungsheft* 540, pp. 16-28, (english version in DLR internal report IB 222-90 A 06, Göttingen, 1990)

Baines, N.C.; Kiock, R.; Lehthaus, F.; Sieverding, C.H.; 1985, "A Comparison of Aerodynamic Measurements of the Transonic Flow through a Plane Turbine Cascade in four European Wind Tunnels", 8th Syposium on Measuring Techniques for Transonic and Supersonic Flow in Cascades and Turbomachines, Genoa, Italy

Bräunling, W., 1985, "Untersuchungen zum Einfluß der Konizität auf die Kennwerte Rotierender Turbinen-Ringgitter im Transsonischen Geschwindigkeitsbereich", *VDI-Forschungsheft* 627, VDI-Verlag, Düsseldorf

Bräunling, W. and Lehthaus, F., 1986, "Investigations of the Effect of Annulus Taper on Transonic Turbine Cascade Flow", *ASME-J. of Eng. f. Gas Turbines and Power*, vol. 108, pp 285-292

Gotthardt, H., 1983, "Theoretische und Experimentelle Untersuchungen an Ebenen Turbinengittern mit Pfeilung und V-Stellung", Dissertation TU-Braunschweig

Graham, D. and Lewis, R.I., 1974, "A Surface Vorticity Analysis of Three-dimensional Flow throught Strongly Swept Turbine Cascades", *I.Mech.E., J.Mech.Eng.Sc.*, Vol.16, No.6, pp. 425-433

Hill, J.M. and Lewis, R.I., 1974, "Experimental Investigations of Strongly Swept Turbines Cascades with Low Speed Flow", *I.Mech. E., J. Mech. Eng. Sc.*, Vol. 16, No.1, pp. 32-40

Kiock, R.,; Lehthaus, F.; Baines, N.C.; Sieverding, C.H.; 1985, "The transonic flow through a plane turbine cascade as measured in four European windtunnels", ASME paper 85-IGT-44, International Gas Turbine Symposium and Exposition, Beijing, China.

Kost, F., 1992, "Stromflächenverwindung in einem Turbinenlaufrad mit konischen Begrenzungswänden", thesis (in preparation), University of Göttingen.

Krain, H., 1987, "Secondary Flow Measurements with L2F-Technique in Centrifugal Compressors", *AGARD, CP 421, on Advanced Technology for Aero Gas Turbine Components*, 69th PEP Symposium, Paris

Lehthaus, F., 1983, "Transonic Inviscid Flow Calculations for Flow Past Swept-Back Plane Turbine Cascades", *Proceedings of the 7th Conference on Fluid Machinery*, Budapest, Hungarian Academy of Sciences, Vol. 2, pp. 494-504

Potts, I., 1987, "The importance of S-1 stream surface twist in the analysis of inviscid flow through swept linear turbine cascades", *Proceedings I.Mech.E., Turbomachinery-Eficiency Prediction and Improvement*, 1987-6, paper C258/87, p. 231

Schodl, R., 1980, "A Laser-Two-Focus (L2F) Velocimeter for Automatic Flow Vector Measurements in the Rotating Components of Turbomachines", *J. Fluid Eng.*, Vol 102, pp. 412-419

Smith, L.H. and Yei, H., 1963, " Sweep and Dihedral Effects in Axial-Flow Turbomachinery", *ASME-J. Basic Eng.*, Vol.85, No. 3, pp. 401-416